Application: Keratoconus

Corneal-thickness spatial profile and corneal-volume distribution: Tomographic indices to detect keratoconus

Renato Ambrósio Jr, MD, PhD, Ruiz Simonato Alonso, MD, Allan Luz, MD, Luis Guillermo Coca Velarde, DSc

PURPOSE: To evaluate whether the corneal-thickness spatial profile and corneal-volume distribution differentiate keratoconic corneas from normal corneas using new tomography parameters.

SETTING: Subspecialty cornea and refractive practice, Fluminense Federal University, Rio de Janeiro, Brazil.

METHODS: Forty-six eyes diagnosed with mild to moderate keratoconus and 364 normal eyes were studied by the Pentacam Comprehensive Eye Scanner. Corneal thickness at the thinnest point and the averages of the points on 22 imaginary circles centered on the thinnest point with increased diameters at 0.4 mm steps were calculated to create a corneal-thickness spatial profile. Corneal volume was calculated within diameters from 1.0 to 7.0 mm with 0.5 mm steps centered on the thinnest point to create the corneal-volume distribution. The percentage increase in thickness and the percentage increase in volume were calculated for each position of the corneal-thickness spatial profile and corneal-volume distribution from their first value. Statistical analysis was done using the Wilcoxon 2-independent-sample test to compare mean levels using S-Plus-4.0 software (MathSoft) and a normal linear model under a Bayesian frame for estimating the mean variation in thickness and volume using the BUGS 0.6 package.

RESULTS: Statistically significant differences were observed between the groups ($P<.05$) in all positions of corneal-thickness spatial profile and corneal-volume distribution and in the percentage increase in thickness and percentage increase in volume between 3.5 mm and 7.0 mm diameters.

CONCLUSIONS: Corneal-thickness spatial profile, corneal-volume distribution, percentage increase in thickness, and percentage increase in volume were different between keratoconic corneas and normal corneas and could serve as indices to diagnose keratoconus and screen refractive candidates. Further studies are necessary to evaluate whether these tomographic indices are more sensitive and specific than the classic Placido-based topography.

J Cataract Refract Surg 2006; 32:1851–1859 © 2006 ASCRS and ESCRS

Keratoconus is a noninflammatory ectatic dystrophy characterized by progressive thinning, steepening, and apical conic protrusion of the cornea. These changes in corneal shape induce irregular astigmatism and myopic shift, causing gradual impairment of vision.[1,2]

Clinical diagnosis of moderate to advanced keratoconus is not difficult because of the presence of irregular astigmatism and the development of classic retinoscopic and biomicroscopic signs such as localized corneal thinning, Fleischer's corneal epithelial iron ring, Munson's sign, Rizzuti's sign, and Vogt's striae. However, the identification of subclinical forms of the disease in patients with normal best spectacle-corrected visual acuity and minimum or no clinical signs is challenging.

The identification of very early forms of keratoconus or forme fruste keratoconus, described by Amsler in 1946,[2] is important for evaluating and following patients considered to have asymmetric or unilateral keratoconus[3,4] and for studying family members of patients with the disease.[5] Nevertheless, the preoperative identification of forme

Published by Elsevier Inc.

0886-3350/06/$-see front matter
doi:10.1016/j.jcrs.2006.06.025

fruste keratoconus is key for screening candidates for refractive surgery.[6] Patients with keratoconus or other forms of ectasia, such as pellucid marginal degeneration, often have poor outcomes and may have progressive ectasia after laser in situ keratomileusis (LASIK) and photorefractive keratectomy.[7–11] Any refractive surgery practice will have many more patients with corneal ectatic dystrophies and other topographic abnormalities than would be expected from the incidence of each of these disorders in the general population. This reflects self-selection because of dissatisfaction with vision correction provided by glasses or contact lenses. Studies suggest that from 1% to 6% of myopic patients who have vision-correction surgery have keratoconus or are suspected of having keratoconus or other forms of corneal ectasia.[12–14]

Placido disk–based corneal topography has been proposed as the most sensitive method to detect ectatic corneal disorders such as keratoconus and pellucid marginal degeneration.[4,5,15,16] Topographic analyses have yielded characteristic clues to the presence of these diseases before the development of clinical signs or symptoms.[17,18] Several indices and artificial intelligence methods, such as the Rabinowitz-McDonnell test, the KISA% index, the Klyce-Maeda-Smolek Expert System, and the corneal navigator, have been developed to help diagnose keratoconus.[2,19–23] These indices have to have a high degree of sensitivity and specificity to detect keratoconus.[20–23] However, false negatives could occur in cases of pellucid marginal degeneration because most of the systems were calibrated for keratoconus.[24]

The measurement of corneal thickness has become an important factor in several clinical situations such as planning and evaluating the results of most types of corneal and anterior segment surgeries, assessing corneal endothelium dehydration, and detecting as an individual risk factor for glaucoma.[14,25–27] There is a large variation in corneal thickness in the normal population.[14,26] Ultrasonic central corneal thickness usually refers to the measurements at the corneal geometric center or at the apex, which is not the thinnest corneal point.[27] Central corneal thickness is useful in identifying corneal thinning disorders such as keratoconus. It is not advised to rely exclusively on ultrasonic pachymetry to exclude or diagnose keratoconus.[27,28] Regional pachymetry has been used, but a pachymetric map is needed to determine the location and value of the cornea's thinnest point for proper calculations of the mathematics of LASIK and other conditions.[27]

Corneal tomography provides 3-dimensional (3-D) reconstruction of the cornea, enabling evaluation of the anterior and posterior corneal surfaces and creation of a pachymetric map. We believe *tomography* is a better term for such diagnostic approaches. It derives from the Greek words *tomos*, meaning slice, and *graphia*, meaning describing. Commercially available corneal tomography systems use at least four methods: horizontal slit-scanning (Orbscan II, Bausch & Lomb), rotating Scheimpflug camera (Pentacam, Oculus), very-high-frequency ultrasound (Artemis, Ultralink), and high-speed anterior segment optical coherence tomography (Visante, Zeiss). Corneal tomography has been proposed to help to identify forme fruste keratoconus at an earlier stage.[29–33]

In this study, we introduce new corneal tomography parameters derived from the Pentacam Comprehensive Eye Scanner to study corneal architecture; that is, corneal-thickness spatial profile and corneal-volume distribution. We also evaluated whether these parameters can differentiate between keratoconic corneas and normal corneas.

PATIENTS AND METHODS

Forty-six eyes of 23 patients (13 women) diagnosed with mild to moderate keratoconus based on classic corneal topography findings[1,2] and 364 normal eyes of 196 patients (97 women) were studied using the Pentacam Comprehensive Eye Scanner. Pentacam software was used to extract the data from each examination and import them into a Microsoft Excel spreadsheet.

Corneal thickness values at the thinnest point were recorded for each eye. The averages of thickness values of the points on 22 imaginary circles centered on the thinnest point with increased diameters at 0.4 mm steps were calculated to create the corneal-thickness spatial profile. The percentage increase in thickness was calculated for each position from the thinnest point using the formula

$$(\mathrm{CT}_{@}x - \mathrm{TP})/\mathrm{TP}$$

where CT is the corneal thickness average at each diameter and x represents the diameters of imaginary circles centered on the thinnest point (TP), which had increased diameters from 0.4 to 8.8 mm.

Corneal volume was calculated within diameters from 1.0 to 7.0 mm with 0.5 mm steps centered on the thinnest point to create the corneal-volume distribution. The percentage increase in volume was calculated for each position from the 1.0 mm volume using the formula

$$(\mathrm{CV}_{@}y - \mathrm{CV}_{@}\ 1.0\ \mathrm{mm})/\mathrm{CV}_{@}\ 1.0\ \mathrm{mm}$$

Accepted for publication June 18, 2006.

From Instituto de Olhos Renato Ambrósio (Ambrósio Alonso) and Fluminense Federal University (Ambrósio, Alonso, Coca Velarde), Rio de Janeiro, and Altino Ventura Foundation (Luz), Recife, Brazil.

Dr. Ambrósio is a consultant to Oculus-Optikgeräte GmbH. No other author has a financial or proprietary interest in any material or method mentioned.

Corresponding author: Renato Ambrósio Jr, MD, PhD, Rua Conde de Bonfim 211/712, Tijuca, Rio de Janeiro-RJ, 20520-050. Brazil. E-mail: renatoambrosiojr@terra.com.br.

where CV is the corneal volume at each diameter and *y* represents the calculated diameters of corneal volume (CV) from 1.0 to 7.0 mm with 0.5 mm steps.

Data from the Excel spreadsheet were exported to S-Plus 4.0 software (MathSoft). Statistical analysis was done to compare each position of corneal-thickness spatial profile, percentage increase in thickness, corneal-volume distribution, and percentage increase in volume in normal corneas and keratoconic corneas using the Wilcoxon 2-independent-sample test to compare mean levels. A normal linear model under a Bayesian frame was used for estimating the mean variation in thickness and volume using the BUGS 0.6 package (http://www.mrc-bsu.cam.ac.uk/bugs/. Accessed August 25, 2006).

RESULTS

Statistically significant differences were observed between the groups ($P<.05$) in all positions of corneal-thickness spatial profile and corneal-volume distribution and in the percentage increase in thickness and percentage increase in volume between the 3.5 mm and 7.0 mm diameters.

Corneal Thickness Spatial Profile

Significant differences were found in all positions of the corneal-thickness spatial profile in normal eyes and keratoconic eyes ($P<.01$); eyes with keratoconus had much lower (thinner) values. It was estimated that keratoconic corneas were a mean of 27.3 μm thinner than normal corneas.

In keratoconic eyes, the mean thinnest point was 428 μm ± 72 (SD) (95% confidence interval [CI] limits, 391 to 474; range 245 to 563 μm). In normal eyes, the mean was 537 ± 36.7 μm (95% CI limits, 513 to 562; range 439 to 630 μm).

For the 4.8 mm circle diameter, the mean thickness of the keratoconic corneas was 536.5 ± 48.3 μm (95% CI limits, 516 to 566; range 377 to 623 μm). In normal eyes, the mean was 589 ± 36.9 μm (95% CI limits, 564 to 614.8; range 467 to 693 μm).

For the 8.8 mm circle diameter, the mean thickness value of the normal corneas was 712.2 ± 50.0 μm (95% CI limits, 677 to 746; range 581 to 657 μm). In keratoconic eyes, the mean was 695.6 ± 54.4 μm (95% CI limits, 667 to 734; range 541 to 797 μm).

Table 1 shows the mean, standard deviation, 95% CI limits, and the minimum and maximum values for the corneal-thickness spatial profile in normal eyes and keratoconic eyes. Figure 1 shows the results in normal and keratoconic eyes for the corneal thickness spatial profile.

Table 1. Corneal-thickness spatial profile in normal and keratoconic corneas. Values are in microns.

CTSP Position	Norm Min	Kerato Min	Norm Mean	Kerato Mean	Norm Max	Kerato Max	Norm SD	Kerato SD	Norm Lower Limit	Kerato Lower Limit	Norm Upper Limit	Kerato Upper Limit
0.0	439.0	245.0	536.5	428.0	630.0	563.0	36.7	72.0	532.7	406.9	540.3	449.0
0.4	440.0	247.0	536.9	429.0	630.0	563.0	36.7	71.5	533.1	408.1	540.7	449.8
0.8	441.0	252.0	538.0	431.9	631.0	565.0	36.6	70.2	534.2	411.4	541.7	452.4
1.2	444.0	260.0	539.8	436.7	632.0	567.0	36.6	68.1	536.0	416.8	543.6	456.6
1.6	447.0	268.0	542.3	443.2	634.0	570.0	36.6	65.5	538.6	424.1	546.1	462.4
2.0	451.0	278.0	545.6	451.3	637.0	573.0	36.5	62.3	541.8	433.1	549.4	469.5
2.4	457.0	290.0	549.7	460.7	640.0	578.0	36.5	59.0	545.9	443.5	553.4	478.0
2.8	463.0	303.0	554.4	471.4	644.0	583.0	36.5	55.9	550.7	455.1	558.2	487.7
3.2	470.0	317.0	560.0	483.0	652.0	589.0	36.5	53.0	556.2	467.5	563.7	498.5
3.6	477.0	331.0	566.2	495.5	661.0	596.0	36.6	50.8	562.4	480.7	570.0	510.4
4.0	484.0	346.0	573.2	508.7	671.0	603.0	36.7	49.3	569.4	494.3	577.0	523.1
4.4	491.0	361.0	580.9	522.3	682.0	611.0	36.8	48.5	577.1	508.1	584.7	536.5
4.8	497.0	377.0	589.4	536.5	693.0	623.0	36.9	48.3	585.5	522.4	593.2	550.6
5.2	504.0	393.0	598.5	551.0	707.0	634.0	37.1	48.8	594.7	536.7	602.3	565.2
5.6	513.0	408.0	608.3	565.7	722.0	645.0	37.5	49.8	604.5	551.2	612.2	580.2
6.0	522.0	424.0	618.8	580.8	737.0	659.0	38.2	50.9	614.9	565.9	622.7	595.6
6.4	531.0	439.0	630.0	596.2	752.0	686.0	39.1	52.2	626.0	580.9	634.0	611.4
6.8	537.0	455.0	641.8	611.9	768.0	710.0	40.4	53.2	637.7	596.3	646.0	627.4
7.2	544.0	471.0	654.4	628.2	784.0	733.0	42.0	54.2	650.0	612.3	658.7	644.0
7.6	553.0	487.0	667.6	644.9	800.0	753.0	43.8	54.9	663.1	628.9	672.1	660.9
8.0	564.0	505.0	681.5	662.2	817.0	770.0	45.8	55.4	676.8	646.1	686.2	678.4
8.4	576.0	523.0	696.4	678.7	836.0	785.0	47.8	55.3	691.5	662.6	701.4	694.9
8.8	581.0	541.0	712.2	695.6	857.0	797.0	50.0	54.4	707.1	679.7	717.4	711.6

CTSP = corneal-thickness spatial profile; Kerato = keratoconic corneas; Lower Limit and Upper Limit = limits for 95% confidence interval; Max = higher value; Min = lower value; Norm = normal corneas

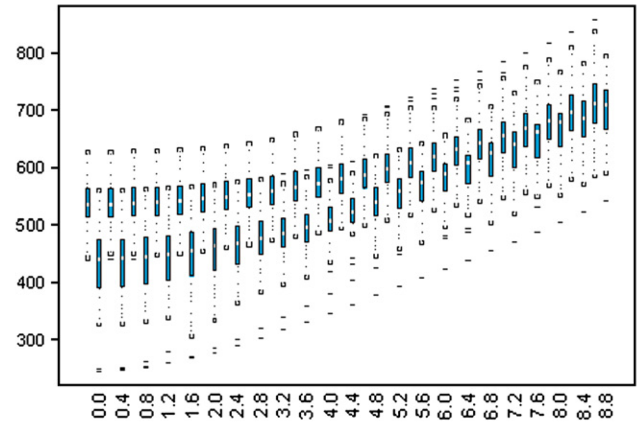

Figure 1. Spatial distribution of thickness values for normal corneas (*first bar*) and keratoconic corneas (*second bar*). The *x*-axis represents the circle diameter centered on the thinnest point (0.0). The *y*-axis represents the mean corneal-thickness values (μm) at each circle.

Normal corneas had a more homogeneous increase than eyes with keratoconus, which was confirmed by the percentage increase in thickness.

Percentage Thickness Increase

Significant differences were found in all percentage increases in thickness in normal eyes and keratoconic eyes ($P<.0001$). The keratoconic eyes had much higher increases.

In keratoconus eyes, the mean percentage increase in thickness for values within the circle diameter of 0.4 mm was 0.27% ± 0.29% (95% CI limits, 0.19 to 0.26; range 0.0 to 1.6%). In normal eyes, the mean was 0.07% ± 0.09% (95% CI limits, 0 to 0.18; range 0.0 to 0.23%).

For the 4.8 mm circle diameter, the mean percentage increase of the keratoconic corneas was 28.2% ± 21.4% (95% CI limits, 13.8 to 34.8; range 6.1 to 129%). In normal eyes, the mean was 9.9% ± 1.9% (95% CI limits, 8.7 to 11.1; range 3.3 to 17.9%).

For the 8.8 mm circle diameter, the mean percentage increase in the keratoconic corneas was 67.7% ± 35.6% (95% CI limits, 47.4 to 74.5; range 24.9 to 221.3%). In normal eyes, the mean was 33.0% ± 7.7% (95% CI limits, 27.1 to 38.6; range 13 to 52.4%).

Table 2 shows the mean, standard deviation, 95% CI limits, and the minimum and maximum values for the percentage increase in thickness in normal eyes and keratoconic eyes. Figure 2 shows the percentage increase in thickness in normal eyes and keratoconic eyes. Normal corneas had a noticeably more homogeneous increase than keratoconic corneas, a finding suggested by the corneal-thickness spatial profile.

Corneal-Volume Distribution

Significant differences were found in all positions of the corneal-volume distribution between normal eyes and keratoconic eyes ($P<.05$); keratoconic corneas had much less volume. It was estimated that keratoconic corneas had a mean volume of 0.943 mm^3 less than normal corneas.

In keratoconus eyes, the mean volume within the 1.0 mm diameter was 0.34 ± 0.06 mm^3 (95% CI limits, 0.3225 to 0.3575; range 0.2 to 0.4 mm^3). In normal eyes, the mean was 0.4 ± 0.43 mm^3 (95% CI limits, 0.4017 to 0.4083; range 0.3 to 0.5 mm^3.

For the 4.0 mm diameter, the mean volume of the keratoconic corneas was 6.14 ± 0.69 mm^3 (95% CI limits, 5.9 to 6.5; range 3.9 to 7.5 mm^3). In normal eyes, the mean was 7.13 ± 0.47 mm^3 (95% CI limits, 6.8 to 7.4; range 6.0 to 8.3 mm^3).

For the 7.0 mm diameter, the mean volume of the normal corneas was 24.5 ± 1.6 mm^3 (95% CI limits, 23.4 to 25.5; range 20.6 to 28.8 mm^3). In keratoconic eyes, the mean was 22.3 ± 1.96 mm^3 (95% CI limits, 21.6 to 23.6; range 15.9 to 25.8 μm).

Table 3 shows the mean, standard deviation, 95% CI limits, and the minimum and maximum values for the corneal volume in normal eyes and keratoconic eyes. Figure 3 shows the corneal volume distribution in normal eyes and keratoconic eyes. Normal corneas had a more homogeneous increase than keratoconic corneas, but this difference was not as evident as with the increase in thickness.

Percentage Volume Increase

The percentage increase in corneal volume did not reach statistical significance for the volumes within the

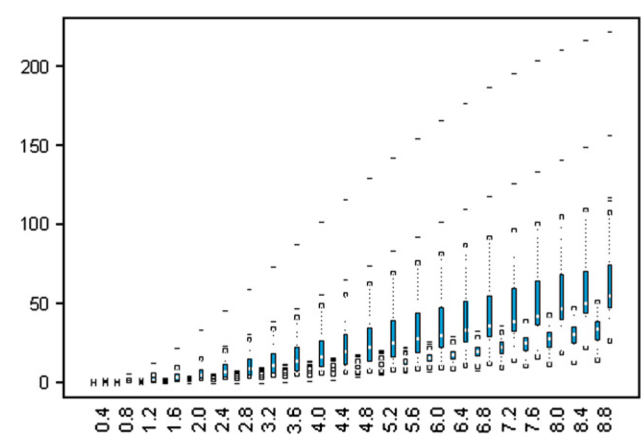

Figure 2. Percentage increase in thickness—spatial distribution of the percentage increase in thickness from the thinnest point for normal corneas (*first bar*) and keratoconic corneas (*second bar*). The *x*-axis represents the circle diameter centered on the thinnest point (0.0). The *y*-axis represents the percentage thickness increase.

Table 2. Percentage of thickness increase in normal and keratoconic corneas. Values are the percentage from the thinnest point.

Thickness Increase Position	Norm Min	Kerato Min	Norm Mean	Kerato Mean	Norm Max	Kerato Max	Norm SD	Kerato SD	Norm Lower Limit	Kerato Lower Limit	Norm Upper Limit	Kerato Upper Limit
0.4	0.0	0.0	0.1	0.3	0.2	1.6	0.1	0.3	0.1	0.2	0.1	0.4
0.8	−0.2	0.2	0.3	1.1	0.8	5.6	0.1	1.0	0.3	0.8	0.3	1.3
1.2	−0.4	0.4	0.6	2.3	1.5	12.5	0.2	2.1	0.6	1.7	0.6	2.9
1.6	−0.6	0.9	1.1	4.0	2.7	21.8	0.4	3.6	1.0	3.0	1.1	5.1
2.0	−0.8	1.5	1.7	6.2	4.0	33.1	0.6	5.4	1.6	4.6	1.8	7.8
2.4	−0.8	2.2	2.5	8.7	5.7	45.6	0.8	7.5	2.4	6.5	2.5	10.9
2.8	−0.8	2.9	3.4	11.5	7.4	58.9	1.0	9.8	3.3	8.6	3.5	14.3
3.2	−0.6	3.6	4.4	14.5	9.4	73.0	1.1	12.1	4.3	11.0	4.5	18.0
3.6	−0.2	4.2	5.6	17.7	11.3	87.5	1.3	14.5	5.4	13.5	5.7	22.0
4.0	0.6	4.8	6.9	21.1	13.4	101.6	1.5	16.9	6.7	16.2	7.0	26.1
4.4	1.7	5.5	8.3	24.6	15.5	115.7	1.7	19.2	8.1	19.0	8.5	30.3
4.8	3.3	6.1	9.9	28.3	17.9	129.0	1.9	21.4	9.7	22.0	10.1	34.5
5.2	5.0	6.9	11.6	32.0	20.1	141.9	2.2	23.6	11.4	25.1	11.8	38.8
5.6	6.1	7.5	13.5	35.7	22.3	154.0	2.6	25.5	13.2	28.2	13.7	43.1
6.0	6.9	8.4	15.4	39.5	25.5	165.7	3.0	27.4	15.1	31.4	15.7	47.5
6.4	7.2	9.6	17.5	43.3	28.9	176.6	3.5	29.1	17.2	34.8	17.9	51.8
6.8	7.7	10.9	19.7	47.2	32.3	186.3	4.1	30.5	19.3	38.3	20.2	56.1
7.2	8.4	12.8	22.1	51.2	36.2	195.6	4.8	31.8	21.6	41.9	22.6	60.5
7.6	9.2	14.9	24.6	55.3	40.1	203.6	5.5	32.9	24.0	45.7	25.2	64.9
8.0	10.4	17.6	27.2	59.5	44.0	210.5	6.3	33.8	26.5	49.6	27.8	69.4
8.4	11.3	21.0	30.0	63.5	48.1	216.5	7.0	34.7	29.3	53.4	30.7	73.7
8.8	13.0	24.9	33.0	67.7	52.4	221.4	7.7	35.6	32.2	57.3	33.8	78.0

Kerato = keratoconic corneas; Lower Limit and Upper Limit = limits for 95% confidence interval; Max = higher value; Min = lower value; Norm = normal corneas

diameters of 1.5 mm, 2.0 mm, 2.5 mm, and 3.0 mm. However, the percentage increase in corneal volume within diameters from 3.5 to 7.0 mm was statistically higher in keratoconic corneas than normal corneas. The statistical significance increased according to the increase in the diameter studied.

For the 3.0 mm diameter, the mean percentage increase in corneal volume of normal corneas was 870% $\pm$ 59.5% (95% CI limits, 825% to 918.8; range 750 to 1033%). In keratoconic eyes, the mean was 891.5% $\pm$ 93.8% (95% CI limits, 800 to 966.7; range 750% to 1150%).

For the 5.0 mm diameter, the mean percentage increase in corneal volume of the keratoconic corneas was 2946% $\pm$ 438% (95% CI limits, 1550 to 3200; range 2350% to 4800%). In normal corneas, the mean was 2737% $\pm$ 172.2% (95% CI limits, 2600 to 2850; range 2375% to 3233%).

For the 7.0 mm diameter, the mean percentage increase in corneal volume in normal corneas was 5969% $\pm$ 381% (95% CI limits, 5675 to 6225; range 5100% to 7200%). In keratoconic eyes, the mean was 6704% $\pm$ 1261% (95% CI limits, 5800 to 7333; range 5025% to 12400%).

Table 4 shows the mean, standard deviation, 95% CI limits, and the minimum and maximum values for the corneal volume in normal eyes and keratoconic eyes. Figure 4 shows the percentage increase in volume in normal eyes and keratoconic eyes. Normal corneas had a more homogeneous and less abrupt increase than keratoconic eyes.

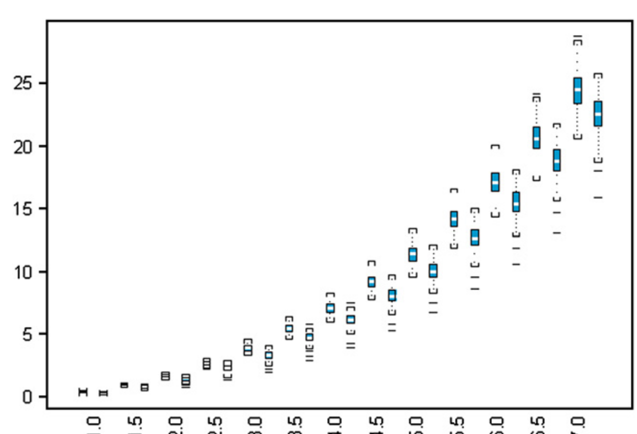

Figure 3. Distribution of corneal volume at different diameters for normal corneas (*first bar*) and keratoconic corneas (*second bar*). The *x*-axis represents the circle diameter centered on the thinnest point (0.0). The *y*-axis represents the volume in each diameter in mm^3.

Table 3. Corneal volume distribution in normal and keratoconic corneals. Values are mm^3.

CVD Diameter	Norm Min	Kerato Min	Norm Mean	Kerato Mean	Norm Max	Kerato Max	Norm SD	Kerato SD	Norm Lower Limit	Kerato Lower Limit	Norm Upper Limit	Kerato Upper Limit
Vol 1.0	0.3	0.2	0.4	0.3	0.5	0.4	0.0	0.1	0.4	−0.1	0.4	0.0
Vol 1.5	0.8	0.5	1.0	0.8	1.1	1.0	0.1	0.1	1.0	−0.2	1.0	0.1
Vol 2.0	1.4	0.8	1.7	1.4	2.0	1.8	0.1	0.2	1.7	−0.4	1.7	0.1
Vol 2.5	2.2	1.4	2.7	2.3	3.1	2.9	0.2	0.3	2.7	−0.6	2.7	0.1
Vol 3.0	3.3	2.0	3.9	3.3	4.6	4.1	0.3	0.4	3.9	−0.9	3.9	0.2
Vol 3.5	4.6	2.9	5.5	4.7	6.4	5.8	0.4	0.6	5.4	−1.2	5.5	0.2
Vol 4.0	6.0	3.9	7.1	6.1	8.3	7.5	0.5	0.7	7.1	−1.6	7.2	0.2
Vol 4.5	7.8	5.3	9.2	8.0	10.8	9.7	0.6	0.8	9.2	−2.1	9.3	0.2
Vol 5.0	9.6	6.7	11.5	10.1	13.4	12.1	0.7	1.0	11.4	−2.6	11.5	0.2
Vol 5.5	11.9	8.6	14.2	12.6	16.6	15.0	0.9	1.2	14.1	−3.2	14.3	0.3
Vol 6.0	14.4	10.6	17.1	15.4	20.1	18.1	1.1	1.4	17.0	−3.9	17.2	0.3
Vol 6.5	17.3	13.1	20.6	18.7	24.2	21.8	1.3	1.7	20.5	−4.7	20.8	0.3
Vol 7.0	20.6	15.9	24.5	22.4	28.8	25.8	1.6	2.0	24.3	−5.6	24.6	0.3

CVD = corneal-volume distribution; Lower Limit and Upper Limit = limits for 95% confidence interval; Max = higher value; Min = lower value; Norm = normal corneas; Kerato = keratoconic corneas; Vol = volume

However, the percentage increase in volume did not reach statistical significance until the 3.0 mm diameter.

DISCUSSION

This study showed that new corneal tomography findings—corneal-thickness spatial profile, corneal-volume distribution, percentage increase in thickness, and percentage increase in volume—are different in keratoconic eyes and normal eyes. Keratoconic eyes have thinner corneas than normal corneas, with less volume and a more abrupt increase in these parameters from the thinnest point toward the periphery.

These findings agree with those in previous reports.[34–39] Mandell and Polse[34] pioneered the investigations of corneal thickness profile in a study using a modified Haag-Streit optical pachymeter with an electronic recording system to document the variation in thickness over the horizontal meridian measured at different angles. In their study, the difference between the central and the peripheral measurements was much greater in eyes with keratoconus; it was most significant at the 35-degree position, where the authors found a difference greater than 0.085 mm as pathognomonic of keratoconus.

Avitabile et al.[35] defined a keratoconus index that evaluated the ratio between the mean peripheral corneal thickness and the thinnest point measured by ultrasound biomicroscopy (UBM). The keratoconus index proved to be very sensitive, detecting significantly different values between normal corneas and keratoconic corneas ($P<.001$, Student *t* test). This also provides a reliable measure of corneal thinning related to the severity of the disease in keratoconic eyes, giving an excellent parameter to use to follow the progression of the disease.[36] This method was semiautomated by Castiglione and Castiglione[37] to speed the computation of the keratoconus index.[37] However, this approach did not become popular in the clinical setting because it is time consuming, difficult to perform, and subjective.[36]

Regional measurements and mapping of corneal thickness are also possible using ultrasound computed tomography single-point measurements.[38,39] However, ultrasound computed tomography does not provide data from the true thinnest point and the angulation of the probe might also account for error in the case of regional thickness measurements. In addition, ultrasound computed tomography does not allow precise localization, even for the central

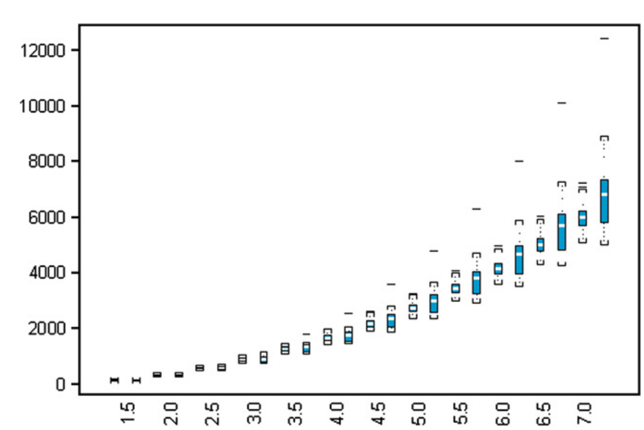

Figure 4. Percentage volume increase from 1.0 mm diameter for normal corneas (*first bar*) and keratoconic corneas (*second bar*). The *x*-axis represents the circle diameter centered on the thinnest point (0.0). The *y*-axis represents the percentage volume increase.

Table 4. Percentage increase in volume in normal and keratoconic corneas. Values are the percentage from the 1.0 mm diameter.

PIV	Norm Min	Kerato Min	Norm Mean	Kerato Mean	Norm Max	Kerato Max	Norm SD	Kerato SD	Norm Lower Limit	Kerato Lower Limit	Norm Upper Limit	Kerato Upper Limit
Dif 1.5	100.0	100.0	138.8	138.2	175.0	166.7	14.6	22.2	137.3	−25.5	140.3	14.8
Dif 2.0	275.0	266.7	321.7	324.1	400.0	400.0	26.5	39.9	318.9	−66.7	324.4	20.4
Dif 2.5	475.0	475.0	569.1	578.7	666.7	700.0	41.1	60.2	564.8	−123.9	573.3	24.0
Dif 3.0	750.0	750.0	870.0	891.5	1033.3	1150.0	59.5	93.8	863.8	−192.9	876.1	37.5
Dif 3.5	1075.0	1075.0	1256.6	1305.7	1466.7	1800.0	82.8	151.7	1248.1	−281.9	1265.2	69.4
Dif 4.0	1425.0	1450.0	1665.4	1749.8	1966.7	2550.0	106.8	218.4	1654.4	−376.6	1676.4	108.3
Dif 4.5	1900.0	1875.0	2186.1	2326.3	2600.0	3600.0	139.1	317.1	2171.7	−495.4	2200.4	172.3
Dif 5.0	2375.0	2350.0	2737.0	2945.7	3233.3	4800.0	172.2	438.3	2719.3	−622.3	2754.8	256.4
Dif 5.5	2975.0	2925.0	3420.3	3725.0	4066.7	6300.0	214.4	597.3	3398.2	−778.4	3442.4	369.8
Dif 6.0	3600.0	3525.0	4145.6	4564.3	4966.7	8000.0	260.3	776.1	4118.8	−943.2	4172.4	500.5
Dif 6.5	4300.0	4250.0	5010.0	5571.9	6033.3	10100.0	315.8	1003.9	4977.4	−1138.5	5042.5	671.3
Dif 7.0	5100.0	5025.0	5968.9	6704.8	7200.0	12400.0	380.7	1261.9	5929.6	−1351.8	6008.1	867.0

Dif = difference; Kerato = keratoconic corneas; Lower Limit and Upper Limit = limits for 95% confidence interval; Max = higher value; Min = lower value; Norm = normal corneas; PIV = percentage increase in volume

point, and proper training is required for reproducible results. Improvement in accuracy for localization of the measurements of the central and peripheral cornea sites is possible but would require a complex apparatus. Owens and Watters[39] describe a system with a Placido disk cone mounted anterior to the slitlamp with the ultrasound computed tomography device mounted on the Goldmann tonometer stand with light-emitting diodes projected on the cornea to help positioning for corneal-thickness measurements. In this study, corneal thickness was negatively correlated with the maximum keratometry reading in eyes with keratoconus, which provides evidence that the thinning process is related to the progression of the disease and could be used for diagnosis and classification.

Pflugfelder et al.[32] suggest 2 indices derived from the corneal-thickness measurements and curvature Orbscan readings. The corneal-thickness index and discriminant function 1 were found to be helpful in distinguishing between eyes of contact lens users and eyes with keratoconus. The corneal-thickness index and discriminant function 1 indices, with respective values of 1.16 or more and −0.60 or less, showed more than 90% specificity and sensitivity in distinguishing patients with true keratoconus from contact lens users and normal subjects.[32] However, this method did not become available, and no further study explored this excellent concept.

We studied the pachymetric distribution or spatial profile using Orbscan IIz data in 2004.[40] In this study, data from 100 normal cases and 25 mild to moderate keratoconus cases was manually extracted using numeric pachymetric maps. A significant difference was found for all positions studied (P>.05, Student t test). However, this method was not automatically implemented in the system. In contrast, a simple ratio of central to midperipheral corneal thickness of 250 μm is proposed.[31]

The Pentacam evaluates the cornea and anterior segment from the anterior corneal surface to the posterior lens surface using a rotating Scheimpflug camera. The noncontact measuring takes approximately 2 seconds and performs from 12 to 50 single captures. A total of 25 000 points are evaluated. Height values are detected and processed to a 3-D model of the anterior eye segment (Figure 5).

An edge detection line can be checked for every image (Figure 5), which increases the confidence in the

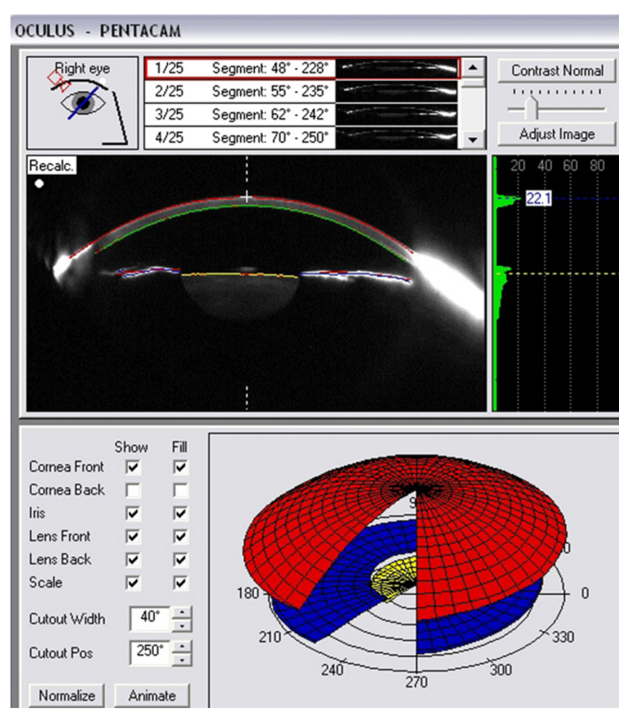

Figure 5. Pentacam cornea and anterior chamber tomography reconstruction.

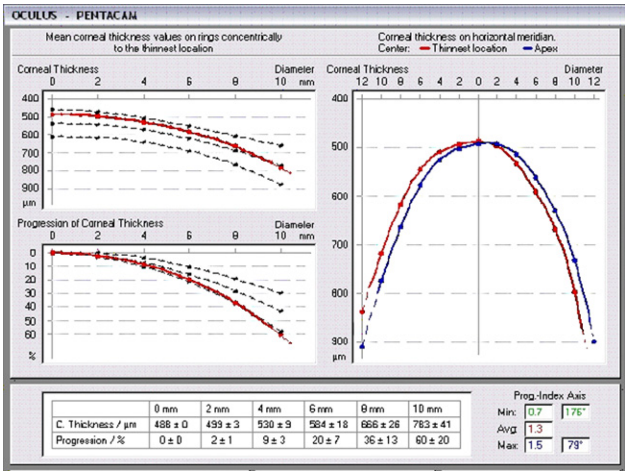

Figure 6. Pentacam screen of the corneal-thickness spatial profile and percentage of thickness increase display (*left*), as well as the corneal thickness on horizontal profile display (red: passing through the thinnest point; blue: passing through the corneal apex-central point) (*right*). This screen is not available on the current Pentacam software. This eye has no evidence of ectasia on corneal surface maps, while the contralateral eye has obvious keratoconus. Note the corneal-thickness spatial profile and percentage increase in thickness are borderline, which suggests this parameter could be more sensitive to detect ectasia.

measurements, especially in corneas with altered transparency. An excellent correlation was found between thickness measurements by the Pentacam and those by ultrasound computed tomography and other methods.[41–43]

Considering the results in our studies, new summaries and graphics exploring data from the pachymetric and volume were developed by the Pentacam software to help clinicians detect ectasia (Figure 6).

This study shows that indices generated from corneal thickness measurements over the entire cornea and calculations of volume can identify mild to moderate keratoconus. This opens new horizons to create artificial intelligence indices for the diagnosis and classification of corneal ectasia. We believe that evaluating the corneal-thickness (pachymetric) map could help differentiate normal thin corneas from ectatic thin corneas (Figure 7).

Currently, most diagnostic and classification criteria for keratoconus are based on anterior corneal curvature data derived from Placido-based corneal topography.[2,15–22] Corneal topography does not evaluate the posterior cornea and the thickness profile and thus misses early ectatic changes. The parameters we describe using corneal thickness and volume should be used in conjunction with the previous ones related to the corneal surface[19–23] to improve the sensitivity and specificity for the detection of very early forms of keratoconus. Several other parameters could be also extracted from corneal tomography examination. These include the location of the thinnest point and difference in the central (geometric) point to the thinnest point. Studies are being performed to test the sensitivity and specificity of the corneal tomography indexes to detect ectasia and to correlate the indices that represent corneal architecture and shape with corneal biomechanical measurements.

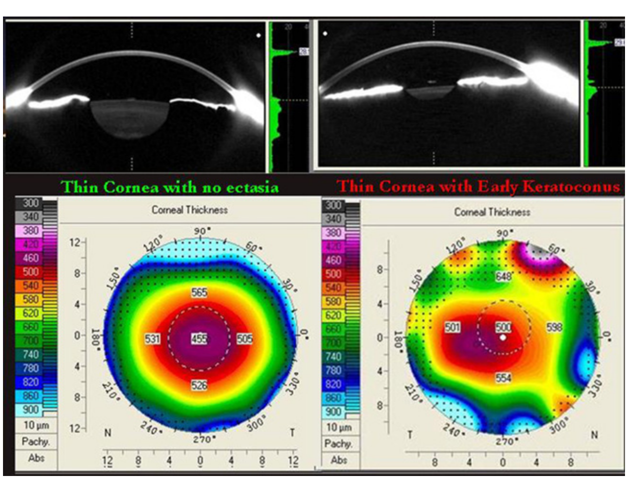

Figure 7. Horizontal Scheimpflug and corneal thickness maps from a normal thin cornea with normal (mild, regular, and symmetric astigmatism on corneal surface) and a forme fruste keratoconus or early keratoconus (with very mild changes on the surface maps, with discrete asymmetry inferior/superior).

REFERENCES

1. Krachmer JH, Feder RS, Belin MW. Keratoconus and related noninflammatory corneal thinning disorders. Surv Ophthalmol 1984; 28:293–322
2. Rabinowitz YS. Keratoconus. Surv Ophthalmol 1998; 42:297–319
3. Holland DR, Maeda N, Hannush SB, et al. Unilateral keratoconus; incidence and quantitative topographic analysis. Ophthalmology 1997; 104:1409–1413
4. Li X, Rabinowitz YS, Rasheed K, Yang H. Longitudinal study of the normal eyes in unilateral keratoconus patients. Ophthalmology 2004; 111:440–446
5. Rabinowitz YS, Garbus J, McDonnell PJ. Computer-assisted corneal topography in family members of patients with keratoconus. Arch Ophthalmol 1990; 108:365–371
6. Ambrósio R Jr, Wilson SE. Complications of laser in situ keratomileusis: etiology, prevention, and treatment. J Refract Surg 2001; 17:350–379
7. Seiler T, Quurke AW. Iatrogenic keratectasia after LASIK in a case of forme fruste keratoconus. J Cataract Refract Surg 1998; 24:1007–1009
8. Amoils SP, Deist MB, Gous P, Amoils PM. Iatrogenic keratectasia after laser in situ keratomileusis for less than v4.0 to −7.0 diopters of myopia. J Cataract Refract Surg 2000; 26:967–977
9. Randleman JB, Russell B, Ward MA, et al. Risk factors and prognosis for corneal ectasia after LASIK. Ophthalmology 2003; 110:267–275
10. Binder PS. Ectasia after laser in situ keratomileusis. J Cataract Refract Surg 2003; 29:2419–2429
11. Binder PS, Lindstrom RL, Stulting RD, et al. Keratoconus and corneal ectasia after LASIK [letter]. J Cataract Refract Surg 2005; 31:2035–2038
12. Wilson SE, Klyce SD. Screening for corneal topographic abnormalities before refractive surgery. Ophthalmology 1994; 101:147–152

13. Nesburn AB, Bahri S, Salz J, et al. Keratoconus detected by videokeratography in candidates for photorefractive keratectomy. J Refract Surg 1995; 11:194–201
14. Ambrósio R Jr, Klyce SD, Wilson SE. Corneal topographic and pachymetric screening of keratorefractive patients. J Refract Surg 2003; 19:24–29
15. Wilson SE, Lin DTC, Klyce SD. Corneal topography of keratoconus. Cornea 1991; 10:2–8
16. Maguire LJ, Bourne WM. Corneal topography of early keratoconus. Am J Ophthalmol 1989; 108:107–112
17. Maeda N, Klyce SD, Tano Y. Detection and classification of mild irregular astigmatism in patients with good visual acuity. Surv Ophthalmol 1998; 43:53–58
18. Ambrósio R Jr, Wilson SE. Early pellucid marginal corneal degeneration; case reports of two refractive surgery candidates. Cornea 2002; 21:114–117
19. Rabinowitz YS, McDonnell PJ. Computer-assisted corneal topography in keratoconus. Refract Corneal Surg 1989; 5:400–408
20. Maeda N, Klyce SD, Smolek MK, Thompson HW. Automated keratoconus screening with corneal topography analysis. Invest Ophthalmol Vis Sci 1994; 35:2749–2757
21. Smolek MK, Klyce SD. Current keratoconus detection methods compared with a neural network approach. Invest Ophthalmol Vis Sci 1997; 38:2290–2299
22. Rabinowitz YS, Rasheed K. KISA% index: a quantitative videokeratography algorithm embodying minimal topographic criteria for diagnosing keratoconus. J Cataract Refract Surg 1999; 25:1327–1335; errata, 2000; 26:480
23. Klyce SD, Karon MD, Smolek MK. Screening patients with the corneal navigator. J Refract Surg 2005; 21:S617–S622
24. Ambrósio R Jr, Klyce SD, Smolek MK, Wilson SE. Pellucid marginal corneal degeneration [letter]. J Refract Surg 2002; 18:86–88
25. Gordon MO, Beiser JA, Brandt JD, et al. The Ocular Hypertension Treatment Study; baseline factors that predict the onset of primary open-angle glaucoma; the Ocular Hypertension Treatment Study Group. Arch Ophthalmol 2002; 120:714–720
26. Flanagan GW, Binder PS. Precision of flap measurements for laser in situ keratomileusis in 4428 eyes. J Refract Surg 2003; 19:113–123
27. Jonsson M, Behndig A. Pachymetric evaluation prior to laser in situ keratomileusis. J Cataract Refract Surg 2005; 31:701–706
28. Rabinowitz YS, Rasheed K, Yang H, Elashoff J. Accuracy of ultrasonic pachymetry and videokeratography in detecting keratoconus. J Cataract Refract Surg 1998; 24:196–201
29. Auffarth GU, Wang L, Völcker HE. Keratoconus evaluation using the Orbscan Topography System. J Cataract Refract Surg 2000; 26:222–228
30. Rao SN, Raviv T, Majmudar PA, Epstein RJ. Role of Orbscan II in screening keratoconus suspects before refractive corneal surgery. Ophthalmology 2002; 109:1642–1646
31. Cairns G, McGhee CNJ. Orbscan computerized topography: attributes, applications, and limitations. J Cataract Refract Surg 2005; 31:205–220
32. Pflugfelder SC, Liu Z, Feuer W, Verm A. Corneal thickness indices discriminate between keratoconus and contact lens-induced corneal thinning. Ophthalmology 2002; 109:2336–2341
33. Huang D. A reliable corneal tomography system is still needed [guest editorial]. Ophthalmology 2003; 110:455–456
34. Mandell RB, Polse KA. Keratoconus; spatial variation of corneal thickness as a diagnostic test. Arch Ophthalmol 1969; 82:182–188
35. Avitabile T, Marano F, Uva MG, Reibaldi A. Evaluation of central and peripheral corneal thickness with ultrasound biomicroscopy in normal and keratoconic eyes. Cornea 1997; 16:639–644
36. Avitabile T, Franco L, Ortisi E, et al. Keratoconus staging; a computer-assisted ultrabiomicroscopic method compared with videokeratographic analysis. Cornea 2004; 23:655–660
37. Castiglione F, Castiglione F. Estimating the keratoconus index from ultrasound images of the human cornea. IEEE Trans Med Imaging 2000; 19:1268–1272
38. Gromacki SJ, Barr JT. Central and peripheral corneal thickness in keratoconus and normal patient groups. Optom Vis Sci 1994; 71:437–441
39. Owens H, Watters GA. An evaluation of the keratoconic cornea using computerised corneal mapping and ultrasonic measurements of corneal thickness. Ophthalmic Physiol Opt 1996; 16:115–123
40. Luz A, Ursulino M, Ambrósio R Jr. Corneal thickness variation from the thinnest point to the limbus: study based in a normal and keratoconus population for creating reference values. Arch Bras Oftalmol 2006; 69:579–583
41. O'Donnell C, Maldonado-Codina C. Agreement and repeatability of central thickness measurement in normal corneas using ultrasound pachymetry and the OCULUS Pentacam. Cornea 2005; 24:920–924
42. Buehl W, Stojanac D, Sacu S, et al. Comparison of three methods of measuring corneal thickness and anterior chamber depth. Am J Ophthalmol 2006; 141:7–12
43. Barkana Y, Gerber Y, Elbaz U, et al. Central corneal thickness measurement with the Pentacam Scheimpflug system, optical low-coherence reflectometry pachymeter, and ultrasound pachymetry. J Cataract Refract Surg 2005; 31:1729–1735